A Programmable Magnetic Field Mass Spectrometer with On-Line Data Processing*

G. J. Wasserburg, D. A. Papanastassiou, E. V. Nenow, and C. A. Bauman
Charles Arms Laboratory of the Geological Sciences, California Institute of Technology, Pasadena, California 91109

(Received 8 July 1968; and in final form, 21 October 1968)

A single focusing, 30.48 cm radius, 60° sector magnet mass spectrometer was constructed with symmetric conjugate foci calculated from fringe field data and corresponding to a beam deflection of 68°. Experimental and calculated optical characteristics agree well. A rotating coil probe and a rate coil are employed as field sensors for a nulling device and for field scanning. The magnetic field can be set to 27 values corresponding to the center of spectral lines and zero lines on both sides of each peak. The automatic scanning consists of: (1) rapid field change between adjacent field values (~500 G/sec); (2) locking in at the preset field values (~0.3 sec); (3) remaining in a channel for a preset time during which the ion beam current is integrated and the data digitized. Repeated arbitrary excursions between channels do not cause effective field variations of more than $|\Delta B/B| = 2\times10^{-5}$. For 0.2 mm source and 0.64 mm collector slit settings, a typical peak at mass 88 is flat for 2.7 G to 0.01% at a 14 kV accelerating potential. Data consist of channel intensity, scale factors, and internally provided clock time; data signals drive a typewriter and tape punch. A cyclic scan of five isotopes including background requires 35 sec. A segment of data (~10 cycles) is processed by the computer and the results returned to the operator.

INTRODUCTION

In measuring the relative isotopic abundances of elements in small samples with high precision we have been limited by the usual analog techniques of data acquisition (e.g., strip chart recorder, slow field scanning). This limitation has been recognized by Moreland, Stevens, and Walling,[1] who designed systems for digital output with voltage scanning combined with a linear magnetic field sweep. This paper will present a system which eliminates chart reading, operator field scanning, and scale switching. The usual slow field scanning to determine accurately the center and intensity of spectral lines is changed to a step scan mode which permits that a greater percentage of time be spent integrating the ion beam intensity and a reduction of errors due to ion beam instability.

The basic aspects of the system are a programmable magnetic field for mass analysis, a digital voltmeter for ion beam integration, and transmission of the data to an on-line computer. The magnetic field can be set to 27 values corresponding to centers of spectral lines and zeros on either side of the peak. Nine channels are completely independent and carry their own identification. In each of the nine main channels the magnetic field may have values $H_k - H_k'$, H_k, and $H_k + H_k''$; these values are selected in sequence in the automatic scan mode and the ion current in each channel integrated. Any channel may be omitted and the cycle may start at any channel. A schematic mass spectrum showing the field values at which data points are taken and possible scanning sequences are shown in Fig. 1; Table I shows the information obtained in each channel. A schematic of the data processing cycle is shown in Fig. 2. Transmission of data to the computer during automatic scanning proceeds at a rate of up to 15 characters/sec for prolonged periods of time. The signals transmitted are stored in sequence on disk and are accessible to programs stored in the computer. A variety of programs for each element and type of experiment is stored and a particular one may be chosen by typing on the Flexowriter; program parameters may also be transmitted from the Flexowriter and interpreted as such,

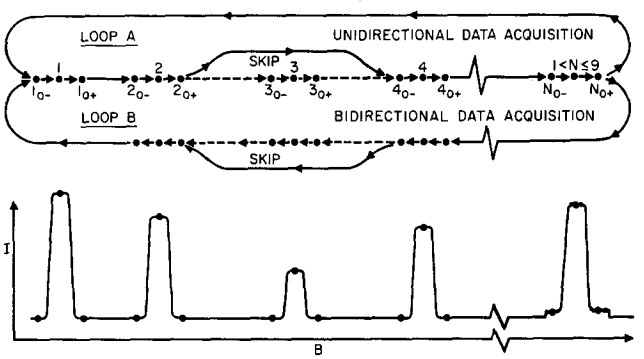

FIG. 1. Magnetic field step scanning. Dots represent field values at which the ion beam is integrated and correspond to points on the mass spectrum shown in the lower diagram. Loops A and B represent unidirectional and bidirectional data acquisition, respectively.

TABLE I. Twenty-seven channel mass analyzer.

a) 9 MAIN CHANNELS. EACH MAIN CHANNEL k IS SET TO 3 FIELD VALUES: $H_k - \Delta H_k'$, H_k, $H_k + \Delta H_k''$, SELECTED IN SEQUENCE IN THE SCAN MODE.

b) DATA OUTPUT AT EACH CHANNEL: ONE 15-CHARACTER WORD.

CHARACTER #		INFORMATION
1	(n)	CHANNEL # / MASS IDENTIFICATION
2-7	(n)	INTEGRATED VOLTAGE (VOLT-SECS)
8	(α)	VIBRATING REED, DIGITAL VOLTMETER, SIGNAL POLARITY
9	(n)	TIME INTERVAL FOR INTEGRATION (1,2,4,8 SECS)
10-14	(n)	TIME AT INITIATION OF INTEGRATION
15	(?)	END OF WORD CODE (TAB)

* Contribution No. 1543, Division of the Geological Sciences.

[1] P. E. Moreland, Jr., C. M. Stevens, and D. B. Walling, Rev. Sci. Instrum. 38, 760 (1967).

distinct from the otherwise continuous stream of data. Processing of the data occurs in blocks of variable length (~several tens of words). The analyzed data are placed in storage at the computer and simultaneously returned to the laboratory on a second typewriter.

DESIGN PARAMETERS

Assuming good ion optical characteristics the critical factors are the ability to center an ion beam in the detector and to change the magnetic field rapidly between programmed field values. For an ion beam width of 0.2 mm and a collector slit of 0.38 mm, the magnetic field stability required is $|\Delta B/B| \leq 5\times10^{-5}$ for a maximum beam translation of 0.025 mm at the detector slit. The corresponding required stability of the accelerating potential is $|\Delta V/V| \leq 1\times10^{-4}$.

The magnetic field scan rate was chosen to provide a short time for field switching with respect to the time needed to obtain ion beam counting statistics of better than 0.1% for a beam of 10^{-12} A (~6×10^{6} ions/sec).

While it is simple to achieve the field stability required at one point in the magnet gap, it is not evident that a field control which monitors the flux locally is sufficient to regulate the final position of the ion beam. This depends on the total path integral of the magnetic field which may be nonuniform due to hysteresis effects during cycling.

MAGNET CONTROL SYSTEM

Figure 3 is a schematic diagram of the function of the control systems. Each channel has a set of five binary coded switches, which, through relays, select a fraction of the reference voltage from a ratio transformer. A permanent reference magnet rotating at 1800 rpm around a coil provides the primary emf for the ratio transformer. The magnet and coil are placed in a thermostatic oven. A

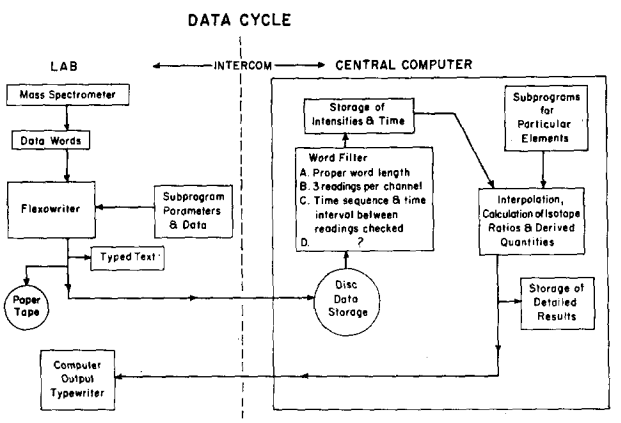

FIG. 2. Block diagram showing data cycle and schematic relationships between spectrometer and on line, time-shared computer (5 min period for set of 10 values of each ratio for five isotopes).

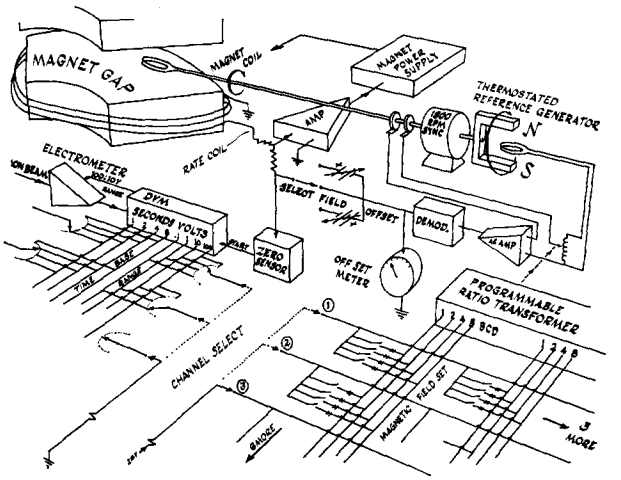

FIG. 3. Schematic of the magnet programming and control system and data acquisition system. A programming panel (not shown) permits (by remote switching) the choice of the numerical values of the magnetic field, time base, DVM, and electrometer ranges for each channel. Upon transfer of data to the memory, the DVM switches channel select (shown as 3) and thus changes the magnetic field set which initiates the slewing mode (see Fig. 4). The zero sensor detects when the new field is achieved and starts the next DVM integration of the ion beam.

second coil extends into the analyzer magnet air gap attached to the end of the same shaft as the rotating permanent magnet. The shaft is placed tangent to the flight tube so that the coil is positioned close to the tube one gap width inside the air gap. The coil is placed along with the shaft and pickup leads in a protective sleeve which has a 6.4 mm diam.

Upon command from the digital voltmeter a new channel is selected which switches in a new fraction of the reference voltage corresponding to a new magnetic field value. This voltage is added to an opposing voltage provided by the rotating coil in the magnet air gap. The resultant emf is amplified and converted to a dc signal by a synchronous rectifier. This signal is applied to an operational amplifier with negative feedback whose output causes the output of the magnet current power supply to change in the signified direction. The current in the magnet changes at a fast rate corresponding to 500 G/sec which we call the slewing mode.

The changing magnetic field creates an emf in the rate coil around the polecap. This voltage is also applied to the operational amplifier and compensates the original signal. At the slewing state the rectifier and amplifier become saturated. Thus the magnetic field overshoots the programmed value and an opposite correction has to be applied by the system, causing some oscillations for a time defined as the "lock in" time (typically ~0.3 sec); thereafter the field remains constant until the next command from the digital voltmeter. The magnetic field as a function of time during automatic step scan is shown schematically on Fig. 4. This system was designed to our

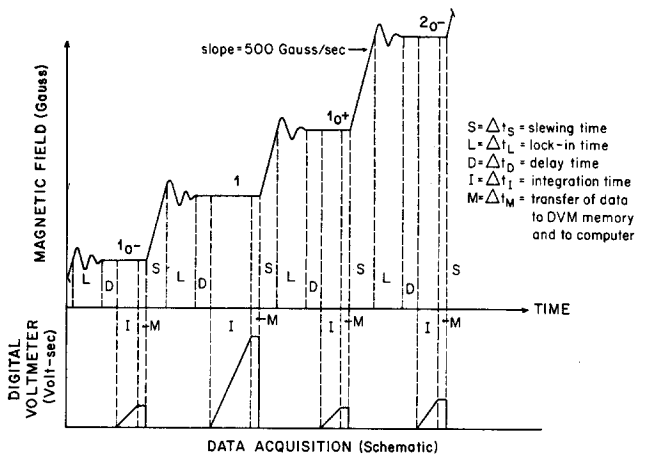

FIG. 4. Magnetic field as a function of time and channel during automatic step scan. The field is switched from channel 1_{0-} to 1, 1_{0+}, 2_{0-}, etc. in the automatic scan mode of Fig. 1. The lower part illustrates the DVM signal. The times involved are as follows (sec): $\Delta t_s \sim 0.04$ for typical jumps in magnetic field; $\Delta t_L \sim 0.3$; $\Delta t_D \sim 1$; $\Delta t_I \sim 1-8$; $\Delta t_M \sim 0.001$. The magnetic field starts to slew automatically when information has been transferred to the DVM one word memory.

specifications by Magnion Inc. using a rotating coil and permanent magnet made by Rawson Inc. An offset voltage supplied by a battery enables us to offset the magnetic field in each channel by up to 10 G on either side of the field setting in the main channel to sample the zeros of each peak. The battery cancels some of the effective rectifier output in such a way that a slightly higher/lower emf from the rotating coil is needed to balance the system. When the step scan is complete, a zero sensor enables the digital voltmeter to start integrating the beam ion intensity for a preset integrating time. At the end of this time interval (Δt_I), the digital voltmeter signals for a change in channel. Scanning is done cyclically and unidirectionally (Fig. 1) to minimize hysteresis effects. By moving the probe in the air gap an optimal position may be found which minimizes hysteresis effects.

DETECTION SYSTEM

The detection system is designed to operate in two distinct modes: (1) pulse counting and (2) analog operation with integration of the ion current using a Faraday cup or an electron multiplier. We will only discuss mode 2. In the analog mode the ion signal is applied to a vibrating reed electrometer (Cary No. 36) with variable feedback resistor (10^{10}, 10^{11}, 10^{12} Ω) with a 0.1 sec time constant for 99% full scale. The output of the electrometer is integrated by a bipolar digital voltmeter for a time interval of 1, 2, 4, or 8 sec. The digital voltmeter (DVM) is equipped with an internal clock with 0.01 sec resolution running continuously from 0 to 1000 sec and recycling. This clock notes and stores the time at the onset of integration. This time is part of the output data and is used for interpolating ion beam intensities. The time intervals of integration, the scale changes on the electrometer (100 V, 10 V), and the DVM range (0.1, 1, 10, 100 V) are provided automatically by a ganged switch which is activated upon entering into a given channel. Each main channel controls its own range and integration interval for maximum sensitivity. In addition, a distinct integration interval may be chosen for the zeros on either side of the peak. In the automatic scan mode a zero sensor initiates the DVM integration after an interval Δt_D from the time the magnetic field is locked in. The interval Δt_D is chosen to avoid any errors due to the time constants for charging up of the system. If the system has an effective time constant τ, the ion beam signal detected will grow exponentially with time from the time the ion beam is switched into the collector. If the signal is integrated for a time Δt_I at a time Δt_D after the beam is in the collector, the resulting measurement will be off the true measurement by a fraction $\epsilon \simeq \tau e^{-\Delta t_D/\tau}/\Delta t_I$. An identical error will be caused by reading the background a time Δt_D after the beam has been switched off the collector; the total error in corrected intensities is thus 2ϵ and depends on how long we wait before integrating the ion signal. To measure this effect we compared the ratios of the ion beam intensities obtained as a function of Δt_D; it was found that $\Delta t_D \simeq 1$ sec reduced any errors to less than 0.01%.

At the end of a DVM reading the output is transferred into the DVM memory and a signal is generated that switches the system to a new channel. While the magnetic field is slewing, the DVM one word memory is typed on the Flexowriter, punched on tape, and the signals transmitted to the computer (Fig. 4). After lock-in at the new channel the zero sensor initiates the DVM integration and the whole process is repeated. The digital voltmeter, the memory unit, and serializer were developed for our re-

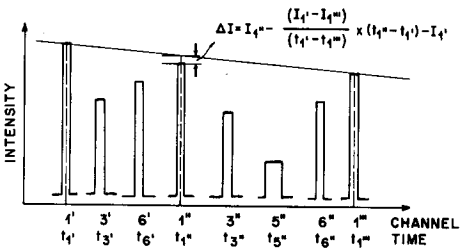

FIG. 5. Interpolation criterion used for calculating isotope ratios. We store in the computer a continuous array of intensities measured, the time of measurement, and the channel identification. Numerals refer to channel numbers and the primes denote successive readings. Channel 1 is here chosen as the index isotope and the criterion is applied to intensities $I_{1'}$, $I_{1''}$, $I_{1'''}$ to calculate ratios in the interval $(t_{1'''}-t_{1'})$. For ratios in the interval $(t_{1''''}-t_{1''})$ we use $I_{1''}$, $I_{1'''}$, and $I_{1''''}$ from the continuous array.

quirements by the Non-Linear Systems, Inc. During scanning each channel may correspond simply to one spectral line, or we may assign more than one channel to a spectral line either for achieving better statistics or for a more complicated background monitoring.

COMPUTER PROGRAM

The IBM 1800 computer is used on a time-sharing basis and is capable of performing all the necessary operations for data reduction. The processing of the data consists of two parts: (a) interpretation of the stream of data and reduction to intensities and time at which readings were obtained and (b) calculation by interpolation of isotopic ratios and of any derived quantities of interest.

In dealing with the continuous stream of data it is found to be more efficient that the data stored on disk be analyzed in small blocks. The natural block size corresponds to data transmitted during one complete step scan cycle, e.g., enough data to calculate one ratio for every isotope measured. In this fashion the computer analysis lags at most one step scan cycle behind the actual data obtained.

To avoid possible errors in the incoming data from being interpreted, a word filter was designed which permits only "legal" words to be used by the programs. The filter checks proper word length; verifies that selected characters are as expected (i.e., α-numeric or numeric); and checks that each data word appears in the proper time sequence, and that the zeros for each peak exist and are in proper sequence (i.e., left zero, peak, right zero). Using the legal data words, the spectral line intensities are calculated by subtracting the appropriate zero intensities and correcting for scale factors and integration times (Δt_I). This information along with the time of onset of integration (corrected for Δt_I) is stored in an array. The members of the array are ordered according to channel number and the time of onset of integration. This order corresponds to the normal sequence of scanning (Fig. 1). Channels which have yielded illegal words or have been accidentally or intentionally skipped during a cycle are stored in this array as zeros. The calculation of isotopic ratios is begun upon accumulation of sufficient data. A self-consistent interpolation criterion has been used as indicated in Fig. 5. We choose a high intensity isotope as an index isotope (e.g., No. 1 in Fig. 5) and calculate the ratios of every isotope to this index isotope. This is satisfactory as long as the index isotope has sufficient intensity to yield good statistics. A more sophisticated system is needed if the precision of the index isotope measurement is poor due to statistics, or if the ion beam is highly unstable or granular. Mean ratios, statistical errors, and derived quantities are calculated in sets of $\sim$10 ratios for each isotope.

Visual beam monitoring is achieved using a recorder (0.2 sec for full scale deflection) in parallel with the digital system with a variable chart speed of 2.54 cm/min to 20.3 cm/sec. The recorder range is controlled by each individual channel being used for optimum sensitivity. To make the visual beam monitoring useful for high precision data, recorder inputs of selected channels are provided with an expanded scale.[2] The magnetic field may also be made to operate in the conventional ramp scan mode in conjunction with analog display on the strip chart recorder.

TABLE II. Beam characteristics.

	(mm)	ΔH equivalent (G)
Potassium		
(B=3500 G at 14.5 kV)		
Source slit	0.2	...
Collector slit	0.69	4.1
Beamwidth	0.2	1.2
Dispersion (per mass unit)	7.62	45
$\lvert\Delta H\rvert_{max}$ (during repeated cycles)	0.013	0.08
$\frac{\lvert\Delta H\rvert_{max}}{H}=2\times10^{-5}$		
Strontium		
(B=5640 G at 16.0 kV)		
Source slit	0.2	...
Collector slit	0.53	5.0
Beamwidth	0.24	2.3
Dispersion (per mass unit)	3.46	32.3

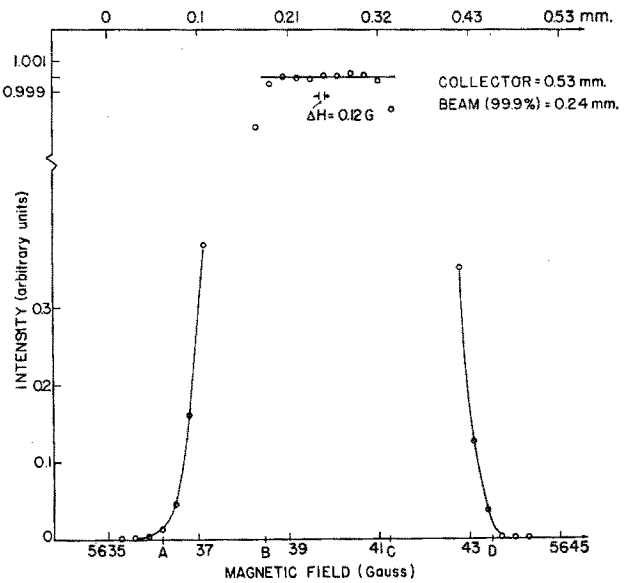

FIG. 6. ^{88}Sr beam profile for collector slit wider than the beamwidth. We obtained intensity readings by changing the magnetic field automatically in small steps, using the mass analyzer. From the distances AB and CD we calculate a beamwidth of 0.24 mm for a 0.2 mm source slit. The gauss equivalent in millimeters is given on the top axis. The signal while the beam is sweeping across the cup is flat to 1×10^{-4} for 2.3 G; beam statistics were a factor of 3 better. The Gauss equivalent scale in millimeters should be multiplied by 2.

[2] W. R. Shields, Nat. Bur. Stand. Tech. Note 277 (1966).

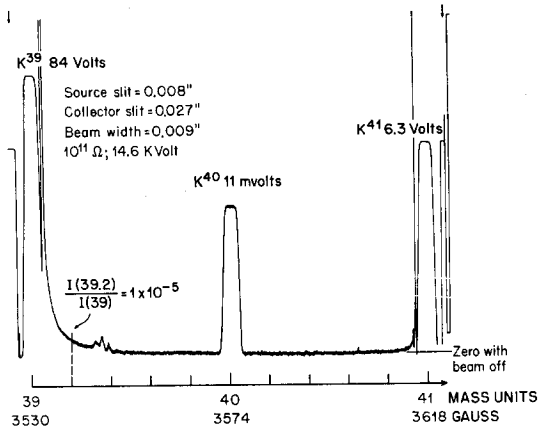

FIG. 7. Potassium spectrum obtained by ramp scanning the magnetic field. Discontinuities in the recorder output correspond to sensitivity changes. The background is very close to the instrument zero shown and remains on the positive side. Small peaks at 39.35 are reflected peaks off a knife-edged baffle.

PERFORMANCE

The operation of the mass spectrometer in the step scan mode depends on our ability to control the magnetic field accurately. In order to determine the reproducibility of the magnetic field settings, we set channels of the magnetic field at the values required to bring a beam halfway in the collector collimating slit. Small instabilities or changes in magnetic field due to repeated cycling thus cause large variations in detected signal intensity.

For this purpose we step scanned cyclically and unidirectionally over the sides and the center of peaks in a potassium spectrum. From the maximum signal intensity changes at the sides of the peaks we find a

$$|\Delta B|_{\max} = 0.08 \text{ G}, \quad \text{or} \quad |\Delta B/B| \leqq 2 \times 10^{-5},$$

during 9 min for 35 cycles. The equivalent maximum drift in the accelerating voltage is $|\Delta V/V| = 4 \times 10^{-5}$. This drift is equivalent to a beam translation in the cup of 0.013 mm.

The accelerating voltage is monitored during an experiment using the DVM and is stable to better than 1×10^{-4} over an hour. A 20 MΩ wire wound resistive divider provides the potentials for the focusing plates in the source. The high voltage is provided by a Walden Co. power supply in the range 10–20 kV at 1 mA maximum load. The unit was modified to eliminate warmup drift by keeping the thermostatic reference ovens on continuously. The power supply can conveniently be modified to provide a programmable high voltage.

Table II shows typical sizes of collimating slits and beamwidths obtained for two elements. Wide collector collimating slits are used; however, they can be narrowed down to the limit defined by the effective field drift. For the thermal ionization source for different experiments over periods of months with slightly different loading and focusing conditions in the source, we find an effective magnetic field drift of 0.3 G. It is, therefore, possible at the beginning of an experiment to choose the magnetic field values in the channels to correspond to the masses under investigation. Thus, even very low intensity signals at known masses may be centered in the collector and data acquisition initiated as soon as signals are detected by the DVM. For signals of sufficient intensity, the center of a peak is determined by finding the average of the two field values at which one-half of the beam is in the detector.

Figure 6 shows the top of a typical spectral line obtained by scanning of the B field in small steps and integrating the ion signal with the digital voltmeter. The observed peak top is flat to better than 1×10^{-4} while the beam traverses the collector collimating slit when the electron suppressor is kept at −180 V. The lower part of Fig. 6 shows the initial increase in signal intensity as the ion beam enters the slit; the distance AB corresponds to a beam image at the collector slit of 0.24 mm width and is very close to the size of the source slit used. Uncertainty $\Delta B/B = 2 \times 10^{-5}$ for locking in at a magnetic field value is shown on the figure and is negligible for beamwidths 0.025 mm narrower than the collector defining slit. The detailed form of beam tails and the possible presence of positive reflected peaks and negative signals due to electrons were investigated by studying the potassium spectrum since $^{39}K/^{40}K = 8 \times 10^3$. A typical spectrum obtained at high beam intensities is shown in Fig. 7. The zero as measured with the beam off is indicated. None of the zero lines and the spectral lines were changed by moving a hand magnet around the tube and in the vicinity of the collector cup and signal lead to the electrometer. The small peaks at mass 39.35 correspond to scattering off a knife-edged baffle placed 3.8 cm in front of the collector slit. At 0.2 m.u. above the center of the mass 39 peak, the intensity has fallen by a factor of 10^5 which corresponds to a tailing of 10^{-5} for peaks separated by 1 m.u. at mass 200. The low mass tail as determined from similar experiments is less than 10% more intense than the high mass tail at symmetric distances from the center of the ^{39}K beam. This condition is obtained using a V-filament (3) and by careful sample loading and focusing in the source.

A study of the characteristics of the mass spectrometer was made by analyzing several samples of strontium extracted from seawater. The sample size ranged from 3×10^{-6} to 5×10^{-9} g of Sr; the latter sample corresponds to 3×10^{-11} g of ^{84}Sr. For each sample load, ratios were obtained as a function of the ion beam intensity in sets of ten during the course of the run. The ratios $^{87}Sr/^{88}Sr$, $^{86}Sr/^{88}Sr$, $^{84}Sr/^{88}Sr$ were measured and the $^{85}Rb/^{88}Sr$ ratio was monitored. To correct for mass discrimination the $^{86}Sr/^{88}Sr$ ratios for each set were used to calculate the discrimination factor by assuming this ratio to be 0.1194; the ratios were then corrected accordingly. Figure 8 shows

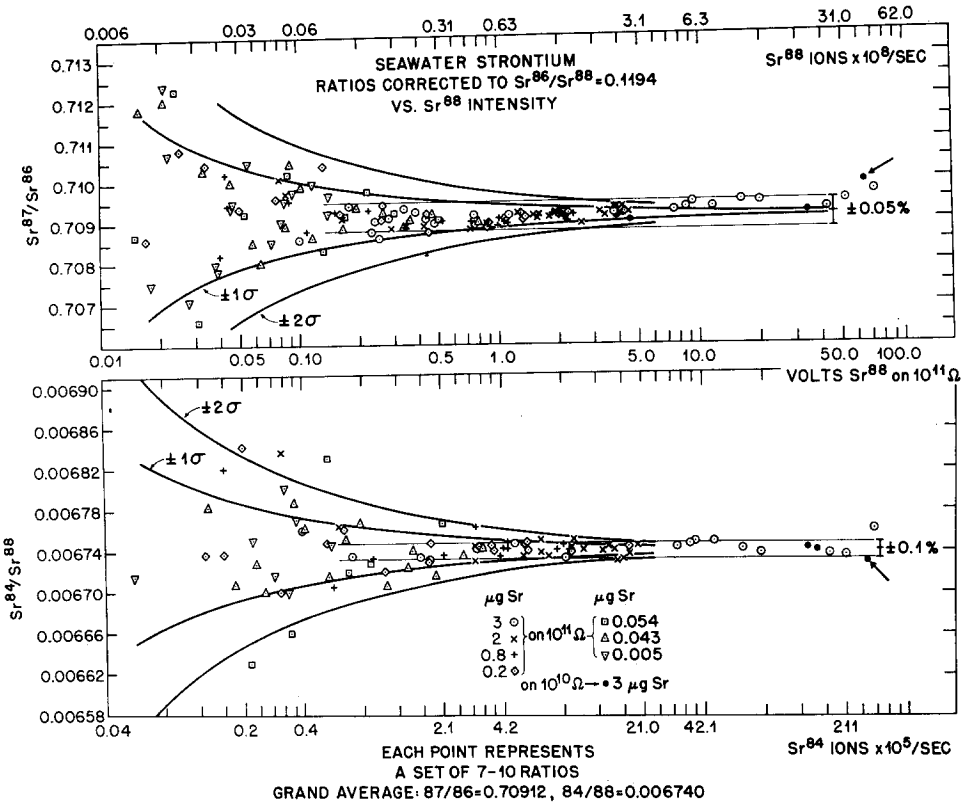

FIG. 8. Isotopic ratios obtained for Sr extracted from seawater as a function of ion beam intensity for samples from 3×10^{-6} to 5×10^{-9} g Sr. Ratios are corrected for mass fractionation. The solid curves represent the expected statistics of the ratios if we assume that statistics are determined by the number of ions. Ratios obtained for ^{88}Sr intensities higher than 10 V on 10^{11} Ω had to be corrected for the voltage coefficient of the resistor which is nonlinear and not well known for high voltages (~50 V). Ratios obtained on the 10^{10} Ω resistor are plotted at the correct ion current but 10× the voltage and did not have to be corrected for voltage coefficient. Two points marked by arrows were obtained during an unstable part of the run while the intensity varied by a factor of 2 (nonmonotonically) in 7 min.

these corrected ratios as a function of beam intensity. It can be seen that for signals ranging from 3×10^{7} to 3×10^{9} ^{88}Sr ions/sec, we obtain ^{87}Sr/^{86}Sr ratios with a total spread less than ±0.05%. From the counting statistics for the number of ^{86}Sr and ^{87}Sr ions collected to form the average of ten ratios, the expected 2σ deviations range from ±0.05% to ±0.005%, correspondingly. At somewhat lower intensities, the data show a wider spread around the average of ^{87}Sr/^{86}Sr=0.70912; this spread is consistent with a $\pm2\sigma$ deviation from counting statistics for the ^{87}Sr and ^{86}Sr. A similar plot for the low abundance isotope ^{84}Sr is shown in the lower part of Fig. 8. In the interval from 6×10^{7} to 3×10^{9} ^{88}Sr ions/sec, the data lie within a ±0.1% band. The counting statistics in this interval determine $\pm2\sigma$ deviations from ±0.1% to ±0.04%. At lower signal intensities the ratios ^{84}Sr/^{88}Sr obtained agree within the $\pm2\sigma$ deviations from counting statistics. At ^{88}Sr intensities lower than 0.05 V, the ^{84}Sr beam was centered in the collec-

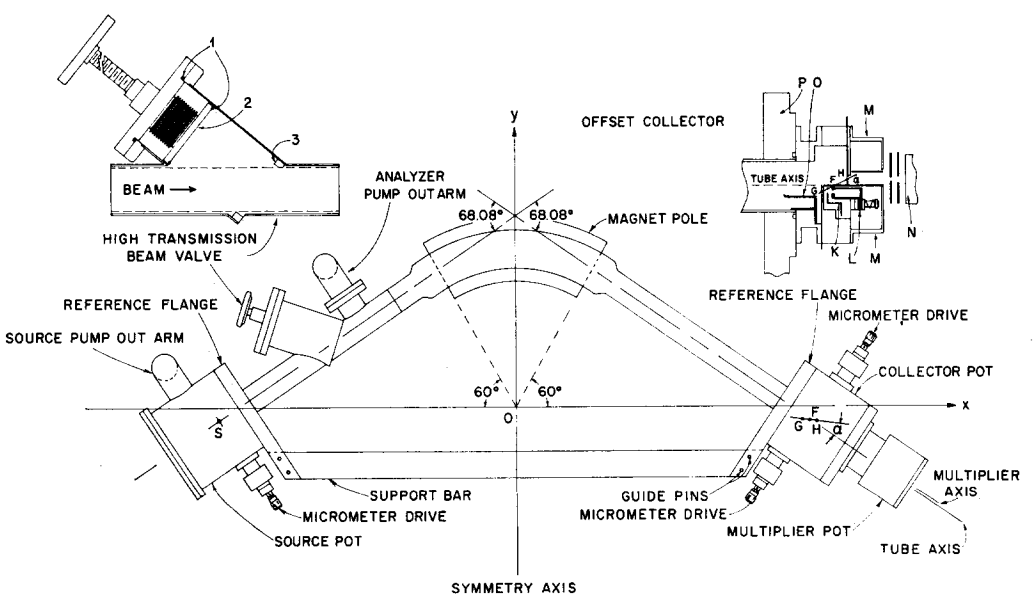

FIG. 9. Schematic drawing of the mass spectrometer. Points S and F are the symmetric foci calculated. The offset collector system is shown in the upper right corner; G and H are the adjustable collimating slits for the simple cup and the multiplier, respectively. K— repeller; L—collector cup; M—shield for simple cup and multiplier; N—multiplier; O—baffle; P—reference flange. Upper left hand shows the beam valve assembly; 1—Viton O rings; 2—valve driver fully retracted; 3—valve seat.

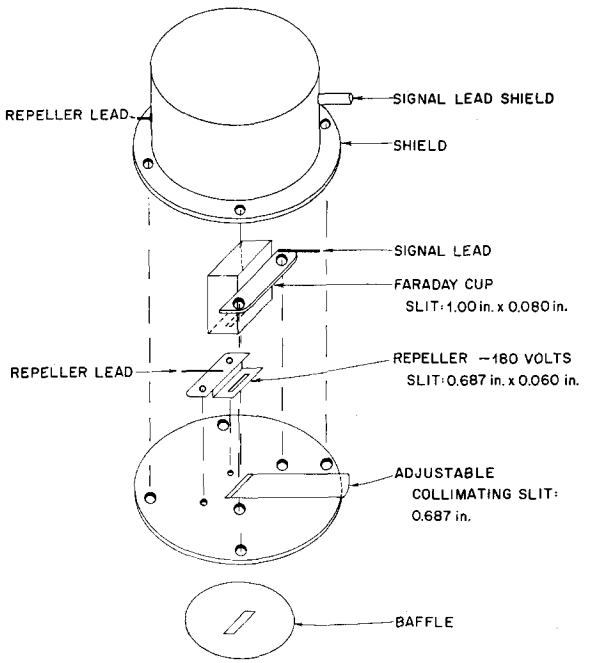

FIG. 10. In-line collector assembly showing complete shield which is placed around the Faraday cup.

tor slit by using the known dispersion of the instrument rather than by watching the analog record. For these Sr experiments we find that the maximum stable beam obtained is proportional to the amount of sample on the filament for this element. For the smallest load of 5×10^{-9} g Sr, we obtained a maximum stable signal of 6×10^{6} ^{88}Sr ions/sec. Measurements were made of isotopic ratios with a beam of 6×10^{3} ions/sec or $\sim10^{-15}$ A for the low abundance isotope. Although this signal is near the noise level of the system, we obtained $\pm10\%$ statistics for the average of 10 ratios by integrating 8 sec at each field value. We conclude that it is possible to obtain $\pm10\%$ statistics with 5×10^{-12} g of a Sr isotope using a Faraday collector.

Very high precision data can be obtained from small samples in short times when we can correct for mass discrimination. When the signal intensity is much greater than the noise level, i.e., for ion currents $\gtrsim7\times10^{-15}$ A, we can obtain results good to within the counting statistics for the number of ions collected by using the digital system and integrating essentially the voltage drop across a resistor. At very high intensities, $\sim10^{-10}$ A, the precision is not improved, even though the counting statistics are better, as we are limited by beam instabilities. For a typical set of 10 ratios we obtain a standard deviation of $\sigma_x\sim0.05\%$. We have observed that if sets of more than 10 ratios are considered, σ_x does not change. Therefore, if the ratios are normally distributed and we obtain approximately 100 ratios (10 sets of 10 ratios) of ^{87}Sr/^{86}Sr, then with $\sigma_x=0.05\%$, the standard deviation of the mean $\sigma_m=0.005\%$ which appears to be the limiting precision of the mean currently available. This is indicated by internal statistics within long runs and by reproducibility of the mean for different runs of the same sample.

DESCRIPTION OF THE INSTRUMENT

A schematic drawing of the mass spectrometer is shown in Fig. 9. The focal points S and F and the beam deflection angle were determined by computer calculations of ion trajectories using the measured magnetic fringe field. A solution was sought with focal points S and F symmetric with respect to the y axis. The coordinates of these focal points are $|x|=58.870$ cm and $y=-2.697$ cm. The beam deflection angle is 68.08° for the 60°, 30.48 cm radius, sector magnetic field used. The line GH is the straight line approximation to the locus of foci and forms an angle $\alpha=26.5°$ with the tube axis. As shown in the upper right hand side of Fig. 9, G is the position of the collimator for the simple Faraday cup and H that for the multiplier.

The construction of the instrument was done with precision of ±0.025 mm over the total length of the instrument for the alignment and positioning of the critical optical elements. The alignment of the tube and reference flanges was done on a boring mill. For this purpose support saddles were placed and screwed into a precision tooling plate on the mill at approximately the proper angles and spacing. These saddles were drilled and bored *in situ* and the tube and beam valve assembly were clamped together; the reference flanges were attached to the tooling plate and locked at the proper relative angles by the 5×5 cm^2 support bar using 12.7 mm guide pins. All welding was performed while the components were clamped. The surface of the reference flanges was finally machined on the boring mill after welding; all distances and angles were measured with reference to the tooling plate and the reference flanges. Alignment holes were bored on the reference flanges on the boring mill and the source and collector assemblies were then mounted using tight guide pins for slit alignment. Stainless steel was used throughout the construction; the tooling plate was made from aluminum and is now used to support the mass spectrometer tube in the horizontal position.

To facilitate magnet alignment the magnet is placed on a cart capable of (a) motion in two orthogonal directions in the horizontal plane and simple rotation in this plane and (b) motion in the vertical direction and tilting off the horizontal plane. The motions in (a) are effected by screw drives, are monitored by indicators, and are easily reproducible to 0.013 mm. The magnet is positioned at its calculated position and the beams obtained are almost theoretical as discussed in the section on performance of the instrument.

The system is differentially pumped by two ion pumps, on either side of the beam valve, which is shown in Fig. 9 in detail; the valve affords full ion beam transmission. Viton O rings are used for gaskets as shown with the O ring

on the driver of the valve out of the ion beam path. Gold and copper gaskets are used for the rest of the machine; a Teflon gasket may be used for the source flange for frequent venting. The analyzer section remains at an equilibrium pressure of 2×10^{-8} Torr as measured at the pump during an experiment; similarly the source section attains a pressure of $\sim5\times10^{-8}$ Torr while running. A Vacsorb pump is used for rough pumping; total pumpdown time is ~15 min for a pressure of 3×10^{-7} Torr after venting the source for sample loading.

A thermal ionization thick lens source with Z-focusing plates is used as designed by Dietz.[3] The final collimating slit is symmetrically adjustable, and the first three plates may be conveniently removed for cleaning after each run.

Two interchangeable collector assemblies have been built for the spectrometer. A schematic plan view of the offset system is shown in Fig. 9. Point G is the collimating slit for the simple cup; this slit is adjustable through a micrometer bellows arrangement. The collector cup is completely enclosed by shield (M) to guard against the electron gas created in the whole region. The signal lead from the cup (not shown here) is also guarded by a cylindrical tube along its path inside the collector pot. The repeller (K) is kept at -180 V and is mounted on a separate insulating stack from the simple cup. The baffle (O) shields the cup from reflected beams and is constructed as a cup to collect most secondaries. The multiplier is also shielded by a can, although complete electron shielding is not as critical.

Figure 10 shows the assembly of a simple in-line cup which may be interchanged with the offset system. In this simpler geometry light tight shielding is easier. Ions and electrons may enter the collector cup only through the collimator slit and the repeller slit which is again kept at -180 V. The beam profiles as discussed before are very good and free of any negative signals or discontinuities in the background resulting from addition of opposite polarity signals.

[3] L. A. Dietz, Rev. Sci. Instrum. **30**, 235 (1959).

ACKNOWLEDGMENTS

The authors wish to thank Pai Young, G. W. Barton, L. A. Dietz, and W. R. Shields for aid and discussion during the design and construction of this instrument. R. E. Haas helped with the computer programming. This research was supported by grants from the National Science Foundation (GP 5391, GP 7976).

THE REVIEW OF SCIENTIFIC INSTRUMENTS VOLUME 40, NUMBER 2 FEBRUARY 1969

Stability of a Current Ring Supported in a Magnetic Field*

V. KELVIN NEIL

Lawrence Radiation Laboratory, University of California, Livermore, California 94550

AND

RICHARD K. COOPER

Physics Department, California State College, Hayward, California 94542

(Received 9 September 1968; and in final form, 24 October 1968)

The stability of a superconducting, current-carrying ring levitated in a static magnetic field is investigated theoretically. The azimuthally symmetric supporting field has components B_r, B_θ, and B_z. A first-order perturbation calculation is performed to determine the oscillation frequencies of the stable modes and the stability criteria for the potentially unstable modes. In the absence of external feedback and/or image currents in the surrounding walls, the ring is unstable. The stability criteria involve the ring current and mass as well as the configuration of the external field and the surrounding walls. It is found that the ring may be stabilized by proper choice of the wall configuration, and if a given configuration is not such as to satisfy the stability criteria, the magnitude of external feedback necessary may be determined from the results.

INTRODUCTION

IN this work we consider the stability of a superconducting ring with major radius R carrying a current I in the azimuthal $(+\theta)$ direction. The ring is supported in a static, externally applied magnetic mirror field **B** as shown in Fig. 1. The field at the ring has a component in the negative z direction. For the ring to be supported against the force of gravity, it must be in equilibrium at a position below the median plane of the external field where there is a small component of **B** in the negative radial direction. In addition, an azimuthal component of the external field can be present. All field components are azimuthally symmetric. The mirror shape of the external field is not essential in the results, which hold for a ring in

* Work performed under the auspices of the U. S. Atomic Energy Commission.